

Article

A Viability Study of Thermal Pre-Treatment for Recycling of Pharmaceutical Blisters

Mertol Gökkelma ¹, Fabian Diaz ², İrem Yaren Çapkın ¹ and Bernd Friedrich ^{2,*}
¹ Department of Materials Science and Engineering, Izmir Institute of Technology, 35430 Izmir, Türkiye; mertolgokelma@iyte.edu.tr (M.G.)

² IME Process Metallurgy and Metal Recycling, RWTH Aachen University, Intzestraße 3, 52056 Aachen, Germany; fdiaz@ime-aachen.de

* Correspondence: bfriedrich@ime-aachen.de

Abstract: Pharmaceutical packaging is one of the most used packaging types which contains aluminum and plastics. Due to increasing amounts of waste and rising environmental concerns, recycling approaches are being investigated. Since blisters usually contain a balanced amount of plastics and metals, most of the approaches focus on recycling only one material. Therefore, more sustainable recycling approaches which recover both plastic and aluminum fractions are needed. This study investigates the thermal behavior and degradation mechanisms of plastic-rich and aluminum-rich pharmaceutical blisters using various analytical techniques. Structural characterization revealed that plastic-rich blisters have a thicker profile with plastic and aluminum layers, while aluminum-rich blisters consist of plastic layers between aluminum sheets. Thermal degradation analysis showed two main stages for both types: plastic-rich blisters (polyvinyl chloride) exhibited significant weight loss and long-chain hydrocarbon formation between 210 and 285 °C, and aluminum-rich blisters (polyamide/nylon) degraded from 240 to 270 °C. Differential Scanning Calorimetry and Fourier Transform Infrared Spectroscopy analyses confirmed the endothermic behavior of such a transformation. The gas emissions analysis indicated an increased formation of gasses from the thermal treatment of plastic-rich blisters, with the presence of oxygen leading to the formation of carbon dioxide, water, and carbon monoxide. Thermal treatment with 5% O₂ in the carrier gas benefited plastic-rich blister treatment, reducing organic waste by up to 80% and minimizing burning risk, leveraging pyrolytic carbon for protection. This method is unsuitable for aluminum-rich blisters, requiring reduced oxygen or temperature to prevent pyrolytic carbon combustion and aluminum oxidation.

Keywords: pyrolysis; thermal treatment; complex scraps; multilayer packages; waste utilization



Citation: Gökkelma, M.; Diaz, F.; Çapkın, İ.Y.; Friedrich, B. A Viability Study of Thermal Pre-Treatment for Recycling of Pharmaceutical Blisters. *Sustainability* **2024**, *16*, 8968. <https://doi.org/10.3390/su16208968>

Academic Editor: Francesco Ferella

Received: 17 September 2024

Revised: 12 October 2024

Accepted: 13 October 2024

Published: 16 October 2024



Copyright: © 2024 by the authors. Licensee MDPI, Basel, Switzerland. This article is an open access article distributed under the terms and conditions of the Creative Commons Attribution (CC BY) license (<https://creativecommons.org/licenses/by/4.0/>).

1. Introduction

Pharmaceutical blister packages are commonly used packaging materials in pharmaceutical manufacturing because of their low price and good protection against moisture [1]. They are also easy to use compared to other types of pharmaceutical packaging (e.g., glass bottles, tubes, etc.). Pharmaceutical blister packages provide easy information about their content as it is possible to print text on the surface, and are a good advertising tool for pharmaceutical companies as they can be easily branded [2]. They are also suitable for the use of solid-form drugs. Drugs in blister packages can be stored separately in airtight spaces.

Pharmaceutical blisters are commonly produced using thermoforming or cold forming methods. Blisters consist of four main components: films, lidding materials, inks, and heat coatings [3]. Plastics such as polypropylene (PP), polyvinyl chloride (PVC), and polyethylene terephthalate (PET) are commonly used to produce forming films. They are used as packaging materials due to their moisture resistance and long-term viability [2]. The lidding properties of aluminum make it a reliable material for drugs to be kept out of the air. Lidding and forming films of cold-formed pharmaceutical blisters are usually

made from aluminum. Compared with thermoforming, cold forming is highly resistant to moisture and light. However, cold forming is a more costly process [3].

Additionally, due to the increasing demand of the pharmaceutical industry, the volume of pharmaceutical packaging waste has increased. Recovering blister packaging is essential to mitigate negative environmental and economic impacts. Currently, there are three main scenarios for end-of-life blister packaging [2], landfill, incineration, and direct recycling, depending on societal policies and attitudes. Plastic and aluminum parts can acidify the soil if landfilled. Additionally, the lack of secondary sources increases primary aluminum production, which is an energy-demanding process [4]. This waste harms the environment and pollutes the air and water [5]. Blister packages containing more plastic are increasingly being assessed as plastic waste because they contain a high amount of plastic and are sent to processes where the metal cannot be recycled. The multilayered structure of pharmaceutical blisters also complicates their recycling, and the separation of the layer might require the usage of chemicals [6].

Pyrolysis is a thermochemical conversion that occurs under anoxic conditions and typically results in no waste, minimal energy, or non-energy consumption. Since pharmaceutical blister packages have a balanced content of plastics and metal, it is difficult to separate both fractions without losing their value. After pyrolysis of waste pharmaceutical blisters, the residue contains both carbonaceous and metallic materials, which can be later recovered using simple metallurgical processes [7].

In the literature, most publications regarding the thermal treatment of pharmaceutical blisters focus on pyrolysis and involve inert media. Kumar et al. graphitized pharmaceutical blisters through pyrolysis, and the product was utilized as an anion material [8]. Parameter optimization can be used to optimize the degradation of polymers into fuels, resulting in higher yields for target products. Klejnowska et al. examined the impact of temperatures on the off-gas composition during the pyrolysis of pharmaceutical blisters [8]. The fuel properties of charcoal obtained from pharmaceutical blister pyrolysis were investigated by Pikon et al. [9]. Although the pyrolysis of blister packages is technically possible, there are still many aspects that need to be addressed to optimize this process and make it economically viable. During pyrolysis, the carrier gas interacts solely with the initial carbon and the developing substances. However, when it comes to pyrolytic gas, the process becomes more complex, leading to variations in the product distribution and char properties [10]. Compared to nitrogen, the CO₂ environment can enhance the product's characteristics and output. It has been proven to enhance the warm productivity of biomass and plastic pyrolysis [11,12].

Currently, most of the aluminum scraps and waste containing organics more than 5% need pre-treatment to reduce the organics levels. Scraps with larger organics result in strong exothermic reactions, which result in uncontrollable temperature levels in the melting stage and increased metal losses due to oxidation [13]. The objective of this study is to explore the potential of thermal pre-treatment with controlled oxygen levels (0–20%) to improve the thermal degradation of organic compounds found in pharmaceutical blisters. By optimizing the quality of the gasses and aluminum products, this approach could enhance their suitability for a more sustainable recycling approach without using the value of both fractions. This research includes a comprehensive analysis of the targeted blister types, as well as a fundamental examination of their thermal behavior, kinetics, and reaction mechanisms during thermal pre-treatment in N₂, N₂ + 5% O₂, or air (20% O₂) atmospheres. Furthermore, this study presents a detailed mass balance of the tested materials.

2. Materials and Methods

Over 1000 pharmaceutical blister packages were collected from pharmacies located in Izmir, Türkiye. Waste blisters were classified according to their type and their brand. In total, plastic-rich (plastic-rich) blister packages with 210 different brands produced by 67 pharmaceutical companies and aluminum-rich (aluminum-rich) blister packages with

66 different brands produced by 32 pharmaceutical companies were used in this study. Figure 1 presents the blisters used in this study for the pyrolysis experiments.

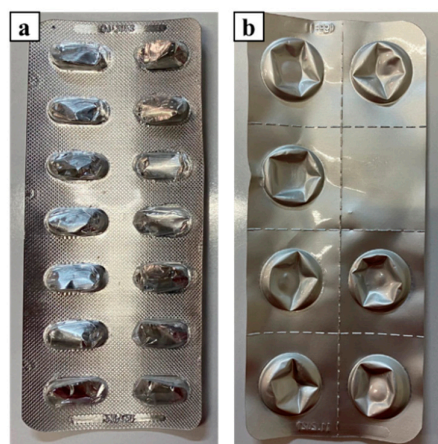


Figure 1. Types of pharmaceutical blisters: (a) plastic-rich, (b) aluminum-rich.

The thicknesses and structures of the aluminum and plastic layers were measured using a Scanning Electron Microscope (SEM) (FEI QUANTA 250 FEG-Oxford Aztec, Hillsboro, OR, USA). For the characterization of the plastic layers, the plastic was shredded to obtain a representative sample which was analyzed by using FTIR (Fourier Transform Infrared Spectroscopy—Perkin Elmer BX Spectrum, Shelton, CT, USA) with a spectral resolution of 4 cm^{-1} and wavenumber range of $4000\text{--}500\text{ cm}^{-1}$, TGA (Thermogravimetric Analysis—Perkin Elmer Diamond) up to $800\text{ }^{\circ}\text{C}$ with a heating rate of $10\text{ }^{\circ}\text{C}/\text{min}$ under N_2 atmosphere, and DSC (Differential Scanning Calorimeter) (Perkin Elmer Diamond) with a heating rate of $10\text{ }^{\circ}\text{C}/\text{min}$ under N_2 gas flow.

Figure 2 shows a schematic of the experimental setup used in the pyrolysis experiments. The experiments were started by loading 5 g of plastic-rich or aluminum-rich blisters, cut in $0.5 \times 0.5\text{ cm}$ pieces, into a sintered aluminum oxide crucible positioned centrally within the reactor. A precision thermocouple was then placed within the crucible to monitor the temperature, with readings recorded at 20 s intervals using a thermologger.

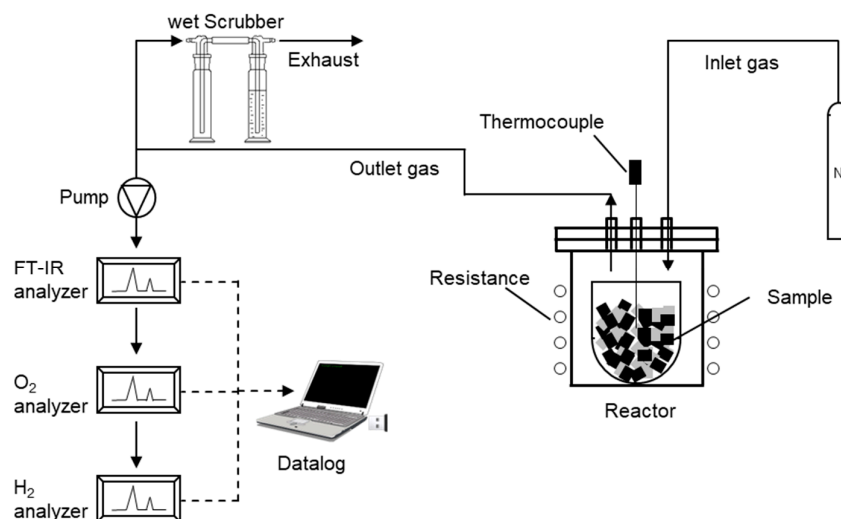


Figure 2. Schematic of the furnace used for laboratory-scale thermal pre-treatment trials.

Subsequently, the reactor was sealed and inserted into a resistance furnace, with insulation provided by glass wool to minimize heat dissipation. The gas inlet and exhaust systems were connected to the reactor and the exhaust was directed through a scrubber unit

designed to collect condensable gasses. Safety precautions were implemented to protect against water flowing into the reactor in the event of pressure loss.

The furnace was programmed to ramp up at a rate of 600 °C/h to a temperature of 800 °C and a dwelling time of 1 h, followed by natural cooling. Throughout the experiment, a continuous flow of N₂, N₂ + 5%O₂, or air (20% O₂) was injected into the reactor at a rate of 6 L/min. Gas sampling, conducted at 2 L/min directly from the reactor, was facilitated by a probe connected to analytical instruments, including FTIR, O₂, and H₂ analyzers, as illustrated in Figure 2. The process parameters were selected according to common practice for laboratory-scale pyrolysis and aligned with the parameters applied to the TGA-DSC.

Gas analysis was performed using a DX4000 FTIR analyzer from Gasmeter, Vantaa, Finland, which can detect various gasses, such as H₂O, CO₂, CO, NO, NO₂, N₂O, SO₂, NH₃, CH₄, HCl, HF, and different volatile organic compounds. The system has a pump that extracts the process gas from the reactor at the above-mentioned rate, fills the measuring cell every 20 s at 180 °C to prevent the condensation during measurement, and releases the measured gas. In this way, the measurement is made continuously, and data is stored every 20 s. Additionally, a PMA 10 paramagnetic O₂ analyzer and LFE Conthos 3E thermal conductivity H₂ analyzer were utilized to detect O₂ and H₂ in vol%, respectively. Each experiment was repeated at least once.

The total volume per component of gas produced during laboratory-scale thermal pre-treatment was calculated by integrating the time–concentration records from the FTIR to obtain the total volumes in normal liters (NI), as shown in Equation (1).

$$V = \frac{1}{d} \sum_{i=0}^n \dot{V} (t_{i+1} - t_i)(c_{i+1} - c_i)/2 \quad (1)$$

where V is the volume of the compound (NI), d is the diluted ratio, \dot{V} is the flow rate of the carried gas (NI/min), c_i is the concentration of the compound at time t_i (ppm), and c_{i+1} is the concentration of the compound at time t_{i+1} (ppm).

3. Results and Discussion

The thickness of all of the collected samples were measured using an electronic caliper. The average thickness of plastic-rich and aluminum-rich blisters were measured as 298.56 µm (±0.036 µm) and 208.04 µm (±0.029 µm), respectively. Figure 3 shows the SEM images, with EDS mapping of plastic- and aluminum-rich blister cross-sections. Plastic-rich blisters have a high volume of plastic layers, shown in blue, and one layer of aluminum between the plastic layers, shown in green. Carbon (shown in red) was observed in the plastic layers due to the C content of plastics. The plastic layers also contained chlorine, owing to the PVC content. The plastic layer is located between the double layers of aluminum in the aluminum-rich blisters.

Figure 4 shows the TGA results of the plastic fractions. The DTG curves showed no weight loss until at least 210 °C, and degradation occurred in two main stages for both the samples. During the TGA analysis of the plastic-rich blisters, the first degradation stage was observed from 210 °C to 285 °C, and the second stage was observed from 375 °C to 455 °C. The first stage indicates the highest degradation rate and is driven by an endothermic process, as indicated by the heat absorption. Moreover, during pyrolysis in the first stage, a tar product is generated, which is then deposited and solidified [14]. The second stage can be explained as being the secondary degradation of the tar generated during the first stage of degradation.

In the temperature range between 285 °C and 375 °C and between 455 °C and 500 °C, the degradation of organics slowed down, and no further degradation was observed after 500 °C. The total mass loss of plastic-rich blisters was 90 wt.%, and the TGA analysis curve matches the TGA results of PVC materials in the literature [15,16].

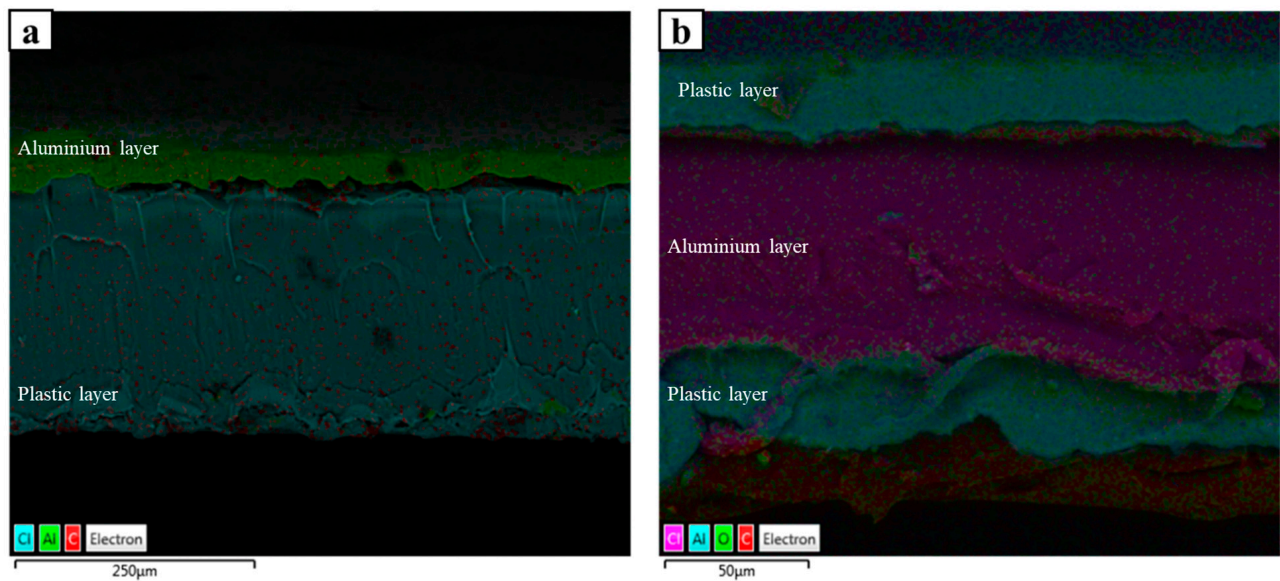


Figure 3. SEM images and EDS mapping of the blisters from the cross-sections of (a) plastic-rich and (b) aluminum-rich blisters.

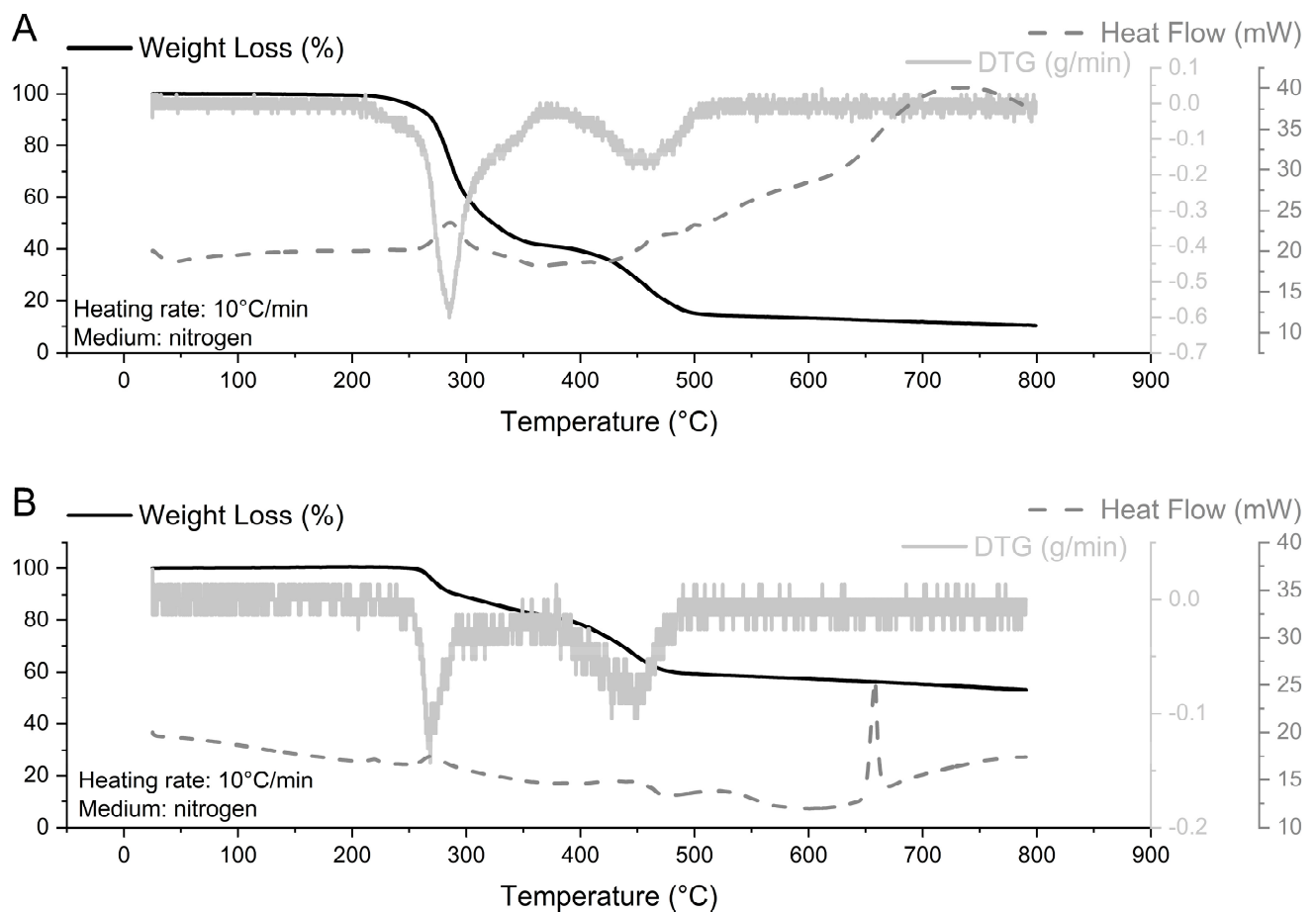


Figure 4. Weight loss, derivative thermogravimetry (DTG), and heat flow during TGA-DSC analysis of thermal pre-treatment of (A) plastic-rich blisters and (B) aluminum-rich blisters.

Figure 4 shows the DSC curves of the plastic fractions of the plastic-rich and aluminum-rich blisters. The DSC analysis for plastic-rich blisters appears to be very similar to the DSC curve of PVC materials, which has several characteristic transitions. PVC is an amorphous polymer that does not exhibit a clear glass transition. However, it shows a gradual increase in the heat capacity in the glass transition region, between 70 and 140 °C. This transition represents a change in the molecular mobility of a polymer.

As shown in Figure 4, the TGA of the aluminum-rich blisters showed two main stages of thermal degradation, but with a slower degradation rate and minimized weight loss compared to that of the plastic-rich blisters. The initial weight loss occurred at approximately 240–250 °C. The second weight loss with a marked change was observed between 380 and 450 °C and could be attributed to the dissociation of the amide bond. The final weight loss could be due to generalized plastic backbone degradation, which occurs between 400 and 500 °C [6,17]. The aluminum-rich blisters mainly consisted of PA/nylon [17], and no significant weight loss was observed at temperatures above 500 °C, indicating that the blister samples were completely decomposed at that temperature.

The DSC results of aluminum-rich blisters show similar characteristics to PA/nylon, which is also a thermoplastic material such as PVC with many characteristic transitions. PA/nylon normally undergoes a melting transition when heated above the crystal melting temperature and then undergoes thermal degradation. The melting temperature of the PA/nylon material in aluminum-rich samples is in the range 260–280 °C [17]. The remainder of the curve describes the behavior of aluminum during heating, including its melting, as depicted by the endothermic peak at approximately 660 °C.

Nylon may thermally breakdown during heating at higher temperatures, as evidenced by a downward shift in the baseline of the DSC curve as an endothermic peak at 260–280 °C, and the generated structure is later degraded again above 380 °C until 450 °C. Both regions indicated an increased DTG.

The pyrolyzed samples (Al- and plastic-rich blisters) were characterized by the presence of aluminum and pyrolytic carbon. The latter is the final product of organic decomposition, which is normally characterized by high C-C bonds and is deposited on the surface of the aluminum foils or found as a fine powder.

As shown in Figure 5 in the FTIR analysis, the plastic fraction of the plastic-rich samples showed characteristic peaks that appeared similar to the PVC spectra measured by Higgins and Jung et al. [18,19]. The spectrum of the adhesive material between the layers (Al and plastic) was very similar to that of the acrylic adhesive spectrum studied by Zieba-Palus et al. [20]. The two groups of peaks located at 2600–3250 cm^{−1} agreed with the asymmetric stretching of HCl [21]. These results are in line with the TGA results, where a strong mass loss at 300–360 °C was observed, supporting the presence of dichlorination. Zhou et al. reported strong absorption peaks between 2600 and 3100 cm^{−1} at 238–409 °C [22,23]. As shown in Figure 5, the C-Cl stretching mode can be observed at 1426 cm^{−1}, CH₂ rocking mode at 1326 cm^{−1}, C-C stretching mode at 1240 cm^{−1}, C-H bending mode at 1096 cm^{−1} and 952 cm^{−1}, and CH₂ bending mode at 614 cm^{−1} for all of the samples. The FTIR spectrum was similar to that of pure PVC reported by S. Ramesh et al. [24]. However, different absorbance peaks were observed, such as the C=O stretching 51 mode at 1632 cm^{−1}, NH bending, and the C-N stretching mode at 1540 cm^{−1} in aluminum-rich blisters. This result shows that the aluminum-rich samples also contained PA/nylon as a plastic fraction, which matched the TGA results. Moreover, minor differences were observed in the FTIR spectra. This may be due to the different adhesive materials used for blisters.

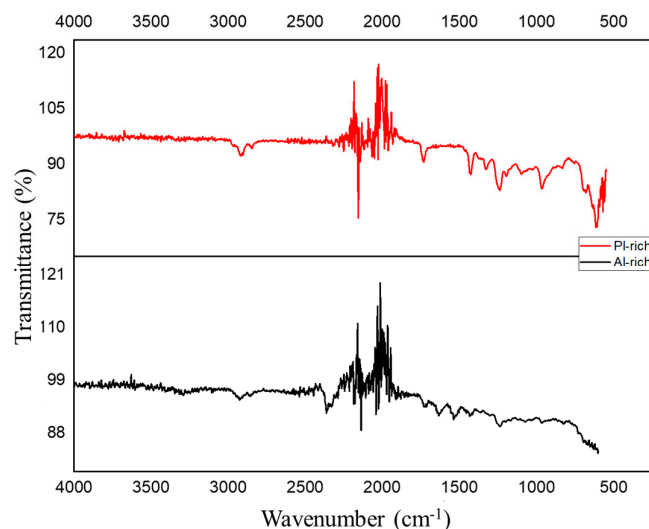


Figure 5. FTIR analysis of plastic fractions of plastic-rich and aluminum-rich blisters.

3.1. Influence of Oxygen during Thermal Degradation

In Figure 6, for all experiments at the set heating rate and variable oxygen concentration, the temperature increased steadily to the target temperature of 800 °C. The consistency of the temperature profile across different oxygen concentrations shows that the thermal conditions were maintained, ensuring that any differences in the gas evolution were due to the chemical environment rather than temperature variations.

In general, like the TGA results, two main degradation phases were observed. However, the peak degradation temperatures shown in Figure 6 are at least 20 °C higher than those indicated by TGA. These slight differences are most likely attributable to variations in the experimental setup.

A clear trend can be observed where the concentrations of certain gasses, such as CO₂ and H₂O, increase with higher oxygen levels and above 200 °C. This finding supports the hypothesis that oxygen facilitates oxidation reactions, leading to the formation of these gasses. It is particularly noteworthy that the increase in CO₂ concentration with higher oxygen levels suggests the complete combustion of the carbonaceous material. The decrease in CO at 580 °C indicates complete combustion and sustained CO₂ generation. The increase in CO₂ and H₂O also increases the oxidation of aluminum, which increases metal losses during thermal treatment.

The presence of various hydrocarbons (e.g., methane, ethane, and propane) under an inert atmosphere (0% oxygen) indicates that pyrolysis is the dominant process. However, their reduced concentrations in the presence of oxygen (5% and 20%) suggest partial oxidation and a shift from pyrolysis to combustion reactions. The online FTIR analysis indicated that the main degradation stage (210–280 °C) in the TG analysis yielded mainly long-chain hydrocarbons, whereas the second one (375–455 °C) yielded mainly oxidation products, as demarked by CO, CO₂, and H₂O compounds.

Pyrolysis oils from plastics require costly halogen removal before use. Therefore, a reduction in oil production during pyrolysis offers economic and environmental benefits [25]. The formation of paraffins, naphthenes, and aromatics in gasses can lead to the production of oils. As shown in Figure 6, the formation of paraffins such as hexane, heptane, and octane generally decrease with an increase in oxygen concentration in the carrier gas during thermal treatment. In the case of cyclohexane, a representative of the naphthene group, its concentration also tends to decrease, but is still detected at 20% O₂. Within the aromatic group, toluene is predominantly present during thermal treatment in the absence of oxygen. The reduction in these compounds in the presence of 5% oxygen suggests that oxidative degradation pathways are prevalent [14]. This is because the reactions with oxygen are stronger than those with hydroxyl radicals, as would occur during pyrolysis in the absence

of elemental oxygen. This effect is relevant because aluminum can be cleaned from pyrolytic carbon without undergoing a strong oxidation effect and avoiding the production of oils, which is normally undesirable owing to the expensive cleaning treatment [25]. Dittrich et al. stated that in the presence of 5 wt.% O₂, a thin protective oxide film immediately forms and hinders the further oxidation of aluminum [26].

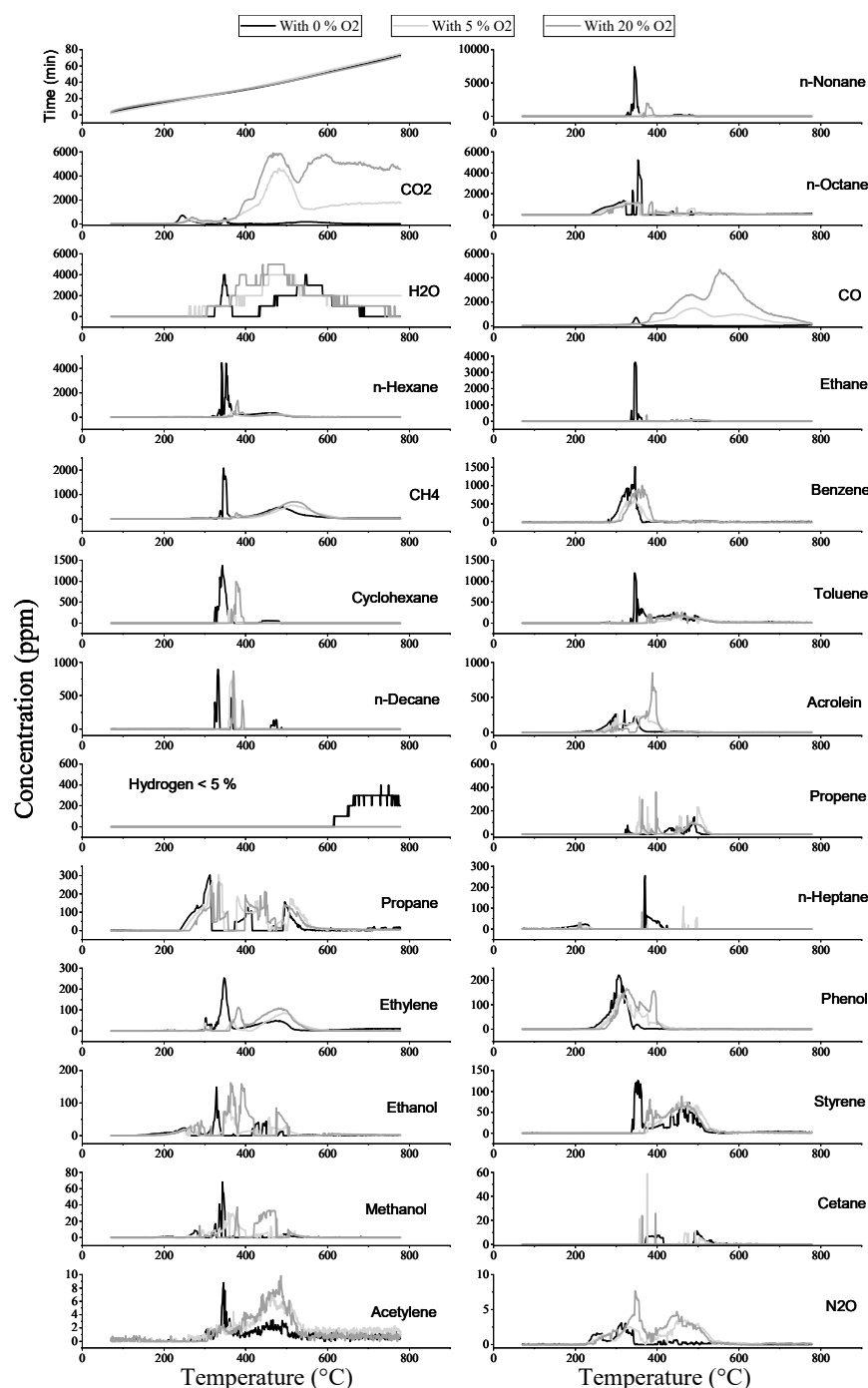


Figure 6. Temperature profile and main species concentration (ppm) during thermal treatment of plastic-rich blisters using 0%, 5%, and 20% oxygen heated at temperatures ranging from 600 °C/h to 800 °C.

The gas concentration profiles show that most compounds peak at approximately the same time as the temperature reaches their maximum, suggesting that the highest rate of gas production coincides with the maximum thermal stress on the material. The

subsequent decreases in concentration are likely due to the consumption of degradable materials and the completion of primary thermal degradation reactions.

The presence of significant amounts of hydrogen (H_2), especially in inert atmospheres, is a common byproduct of the pyrolytic breakdown of organic materials [25]. The influence of oxygen on hydrogen production is noteworthy, as it is no longer detected in Figure 6 in trials with 5% and 20% O_2 . This suggests that, even if hydrogen could potentially form during hydrocarbon degradation, it may be oxidized to form H_2O or not formed at all during the cracking phase, and H_2O may be detected as a product of oxidative reactions with the generated hydrocarbons (C_xH_y). Figure 6 shows evidence of H_2O formation; however, there is insufficient evidence to fully understand the exact pathway of this process. In this context, understanding the formation of H_2 and H_2O during pyrolysis is a topic for further research, as it could have a positive impact by offering an alternative method for “grey hydrogen” production for energy use in an inert atmosphere, or a negative impact due to undesired aluminum oxidation in the presence of H_2O .

The production of NO_x gasses is minimal in an inert atmosphere, but becomes detectable at 5% oxygen and significantly more-so at 20% oxygen. This is a critical point of discussion because NO_x gasses have important environmental and health implications. This is relevant because of the high amount of organic matter in plastic-rich blisters.

The data suggest that, at lower oxygen concentrations, particularly in an inert atmosphere (0% O_2), long-chain hydrocarbons such as n-hexane, cyclohexane, and n-decane are present. These compounds are likely formed due to the thermal breakdown of complex polymers within the blister material. This observation is consistent with a previous study on the pyrolysis of various organic waste materials which suggested that the presence of oxygen decreases the formation of long-chain hydrocarbons and increases the formation of short-chain molecules [27]. Additionally, it results in the increased formation of combusted products such as CO_2 and H_2O .

The introduction of oxygen into the system seemed to facilitate the breakdown of long-chain hydrocarbons into simpler molecules, as evidenced by the decreased concentration of such hydrocarbons at higher oxygen levels. Furthermore, an increased concentration of oxygen leads to the enhanced formation of CO_2 , which can cleave hydrocarbon chains, resulting in the formation of alkanes, benzene, olefins, and HCl , as reported by Wang et al. [7].

Figure 7 presents a detailed account of the gas emissions from the aluminum-rich blisters during thermal treatment in atmospheres with 0, 5, and 20% oxygen. In general, a similar discussion of the degradation mechanisms can be made for aluminum-rich blisters. However, a remarkable observation from this figure is the relatively lower total volume of gasses produced compared to plastic-rich blisters, suggesting a composition that is less prone to volatilization and the increased presence of metals.

When it comes to NO_x , a higher concentration of oxygen can lead to an increased formation of NO_x . However, in the case of aluminum-rich blisters, the results indicate a more stable formation of such compounds, compared to plastic-rich blisters, during the whole temperature range. The only explanation for this phenomenon could be the increased concentration of nylon in the case of aluminum-rich blisters compared to that of plastic-rich blisters, which is predominantly made of PVC.

In Figure 7, the gas profile also shows that while there is an increase in the production of certain gasses with the addition of oxygen, this increase is not as pronounced as might be expected given the variation in the oxygen concentration. Additionally, compared to the plastic-rich blister, CO_2 reaches zero at 20% O_2 above 750 °C, indicating the complete combustion of carbon in the sample. It is worth noting that 5% O_2 still results in a small amount of CO_2 formation, suggesting that carbon remains in the sample and that combustion is hindered by kinetic factors due to the highly packed C-C bonds.

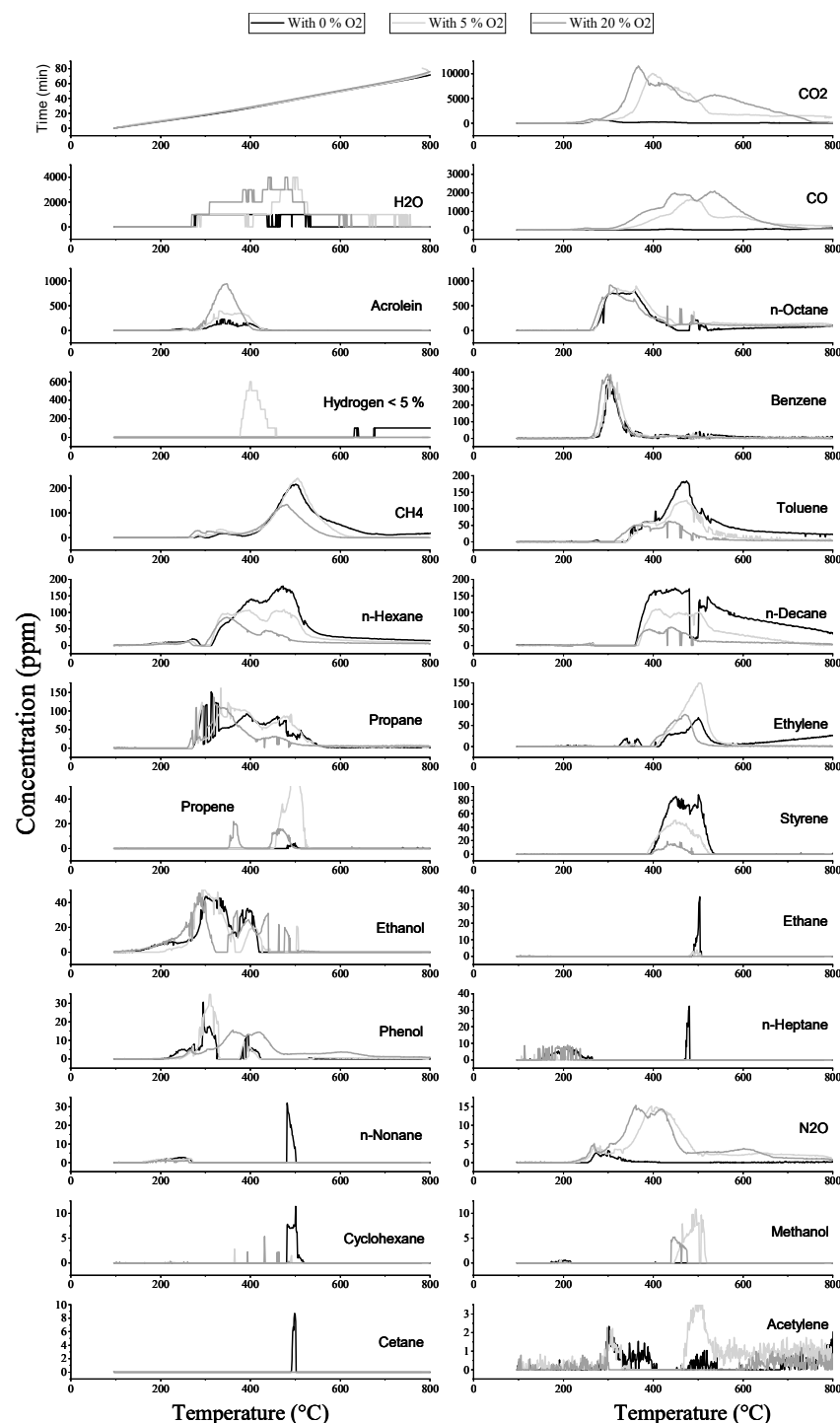


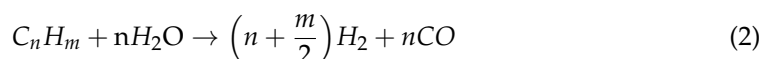
Figure 7. Temperature profile and main species concentration (ppm) during thermal treatment of aluminum-rich blisters using 0%, 5%, and 20% oxygen heated at temperatures ranging from 600 °C/h to 800 °C.

Moreover, the presence of hydrogen generated in aluminum-rich blisters when exposed to 5% oxygen presents a notable divergence from the behavior of plastic-rich blisters. As illustrated in Figure S1, hydrogen formation in aluminum-rich blisters occurs concurrently with the production of long-chain hydrocarbons. Given the higher aluminum content in aluminum-rich blisters, as reported by Diaz et al. and Scholz et al. [14,28], it is plausible that catalytic reactions facilitated by aluminum, especially in molten conditions, enhance hydrogen production via methane cracking. In this context, no references were found in

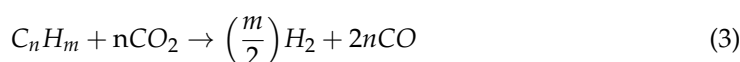
the literature specifically using aluminum, but other metals [29] and aluminum oxide [30], which are known to form a protective layer on aluminum foils, have been studied. More research is needed to understand the catalytic effect of aluminum in both solid and liquid states to form hydrogen from aluminum foils.

The chemical mechanisms contributing to hydrogen generation could include the breakdown of ethane, as suggested by [14], methanation reactions [31], along with methanation and water–gas shift reactions [31,32]. Furthermore, the incorporation of metals such as aluminum and nickel in aluminum-rich blisters may catalyze reactions such as the water–aluminum reaction and steam and dry reforming processes in Equations (2) and (3), respectively. These catalytic processes can lower the temperature threshold required for the cracking of hydrocarbons, as detailed by [13,26], indicating a more complex interplay of thermal and catalytic degradation pathways in aluminum-rich blisters.

Catalytic steam reforming reaction [31]:



Catalytic carbon dioxide (or dry) reforming reaction [31]:



A comparative analysis of the total volume of compounds produced during the thermal treatment of phosphorus-rich (plastic-rich) and aluminum-rich (aluminum-rich) blisters under three different oxygen concentrations, 0%, 5%, and 20% O₂, can be seen in the annexed data depictions.

3.2. Mass Balance

During pyrolysis, the mass of the input material is transferred to the pyrolyzed char or solid residue and the pyrolysis gasses. In this context, pyrolysis gasses are also referred to as the mass of material classified as volatile, which is considered a “Weight loss” in the context of aluminum recycling. Figure 8 shows that weight loss for both blister types increases with higher oxygen concentration, promoting the oxidation and decomposition of pyrolytic coke.

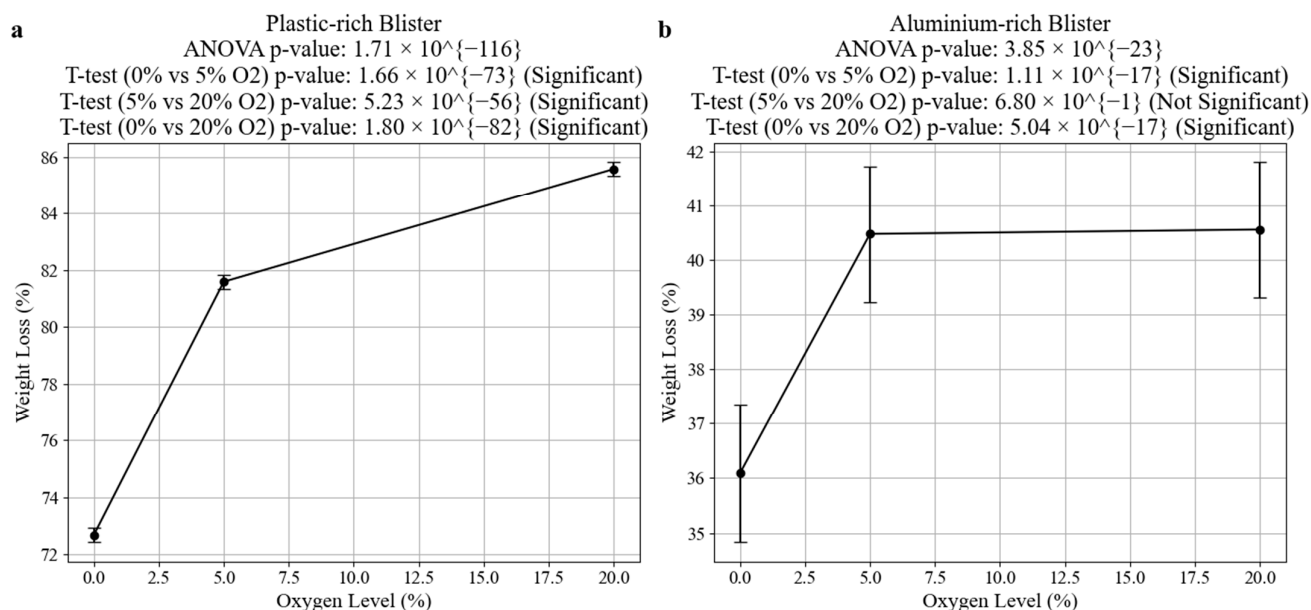


Figure 8. Weight loss after thermal treatment of (a) plastic-rich and (b) aluminum-rich blisters with 0, 5, and 20% O₂.

For aluminum-rich blisters, the *t*-test *p*-values indicate significant weight loss changes between 0% O₂ and 5% O₂ and between 0% O₂ and 20% O₂. However, the change between 5% O₂ and 20% O₂ is not significant, suggesting minimal remaining carbon. The lower weight loss in the aluminum-rich blisters, as indicated in Figure 8, when compared to the gas emission profiles shown above (Figures 6 and 7), provides a supporting view of its thermal degradation behavior and the amount of volatile matter. The reduced generation of gasses such as CO₂ and CO, even in the presence of oxygen, could imply a material matrix that is inherently more resistant to thermal oxidative breakdown, or simply that the availability of carbon-containing compounds is limited in the material.

For plastic-rich blisters, significant weight loss changes are observed between 0% O₂ and 5% O₂ and between 0% O₂ and 20% O₂. The change between 5% O₂ and 20% O₂ is also significant, indicating that increasing oxygen concentration continues to affect weight loss. As expected, the presence of oxygen would promote oxidation reactions, leading to a greater degree of decomposition of pyrolytic coke and, hence, a higher weight loss. Moreover, it is evident that the thermal treatment of plastic-rich blisters with low oxygen concentrations offers advantages. The existence of a possible kinetic barrier in the gasification of carbon at lower temperatures could allow for a controlled process that facilitates the smelting of aluminum without reaching high temperatures, thereby reducing unwanted oxidation of this metal, as the pyrolytic carbon would protect the aluminum layer during smelting and promote sustainability by reducing metal losses.

3.3. Metallurgical Assessment

The metallurgical recovery of aluminum containing organic waste has been extensively discussed in the past for aluminum with organic coatings [6]. However, the application of this knowledge to pharmaceutical blisters presents challenges due to the high organic content.

In this context, the ideal approach would be to perform thermal pre-treatment to reduce the organics without leading to the oxidation of aluminum, leaving an input material that can be incorporated into conventional aluminum recycling operations. According to the results, it is suggested that a pre-treatment with a limited presence of oxygen (4–5%) and a temperature of around 550 °C could sufficiently remove organics from both pharmaceutical blister types (plastic-rich and aluminum-rich), potentially allowing for a unified treatment process. This method avoids the risk of uncontrollable combustion and maintains a lower temperature in the material during organic cracking. The system behaves endothermically under pyrolysis conditions, thereby sustaining reducing atmosphere and preventing undesired aluminum oxidation. The reasons behind this assessment are reported in previous studies on the effect of gasses from organic degradation in melting operations [13,26]. Reduced organics and increased C-C bonds in the pyrolytic coke formed during thermal degradation, compared to untreated organic matter, lack oxygen and hydrogen in their organic structure. Therefore, a reduced oxygen partial pressure marked by reduced CO₂ and H₂O presence in the system would be expected. Consequently, minimized dross formation and higher aluminum yield should be anticipated.

Despite the positive prognosis, a dedicated study on the metallurgical recycling of thermally treated pharmaceutical blisters should be conducted.

4. Conclusions

This study investigated the thermal behavior and degradation mechanisms of plastic-rich and aluminum-rich blister samples using various analytical techniques. Structural characterization revealed distinct differences between the two blister types, with plastic-rich blisters showing a thicker profile and a combination of plastic and aluminum layers, while aluminum-rich blisters had plastic layers sandwiched between aluminum sheets.

The thermal degradation analysis indicated two main stages of degradation for both blister types. Plastic-rich blisters, primarily composed of PVC, exhibited substantial weight loss, endothermic phase transitions, and remarked formations of long-chain hydrocarbons at temperatures between 210 and 285 °C, while aluminum-rich blisters displayed stages

corresponding to the degradation of PA/nylon, indicating a strong degradation period from 240 to 270 °C. Differential Scanning Calorimetry provided further insights into the thermal behavior, revealing characteristic transitions consistent with PVC in plastic-rich blisters and PA/nylon in aluminum-rich blisters.

The FTIR analysis confirmed the presence of PVC in plastic-rich blisters and PA/nylon in aluminum-rich blisters, supporting the compositional analysis. The gas emissions analysis demonstrated differences in gas composition, with plastic-rich blisters producing more gasses. The present study concluded that oxygen, even at a low concentration, could lead to the strong generation of CO₂, H₂O, and CO. Longer-chain hydrocarbons decrease with rising oxygen levels, while hydrogen is detected, even with 5% oxygen, in aluminum-rich blisters, possibly due to the catalytic effects of metallic molten aluminum. Other compounds are present in minor concentrations.

The results evidence that the thermal treatment of plastic-rich blisters would benefit from a low concentration of oxygen, decreasing the organic concentration in the waste by up to 80%, and drastically reducing the surface burning risk in melting operations, reducing dross formation and resulting in a higher recovery yield, thus enabling a more sustainable recycling process. This process takes advantage of pyrolytic carbon, which acts as a layer protecting against the oxygen's interaction with the metal and the reduced involvement of CO₂ and H₂O gasses during melting. However, this method would not be applicable to solely aluminum-rich blisters under the tested conditions, as either the oxygen concentration or the temperature would need to be decreased to avoid the complete combustion of the pyrolytic carbon, risking aluminum oxidation. In this case, blending plastic-rich and aluminum-rich blisters could help maintain a unified treatment process and simplify general recycling operations. Alternatively, aluminum-rich blisters can be recycled after a pre-treatment that separates the layers, as proposed in previous research [7].

Future research could explore additional factors influencing the degradation behavior of blister materials, such as temperature ramp rates, pressure, and moisture content. Further investigation into the catalytic effects of aluminum and other metals present in blister materials could indicate new degradation pathways and opportunities for improved recycling technologies, aiming for better quality of the pyrolysis gasses.

Supplementary Materials: The following supporting information can be downloaded at: <https://www.mdpi.com/article/10.3390/su16208968/s1>, Figure S1: Total Volume of compounds generated during thermal treatment of (A) Pl-rich, (B) Al-rich blisters.

Author Contributions: M.G.: Conceptualization, Methodology, Investigation, Data Curation, Writing—Original Draft, Writing—Review and Editing, Supervision, Project administration, Funding acquisition, F.D.: Conceptualization, Methodology, Investigation, Data Curation, Writing—Original Draft, Writing—Review and Editing, Visualization, İ.Y.Ç.: Methodology, Investigation, Data Curation, Writing—Original Draft, Writing—Review and Editing, B.F.: Conceptualization, Supervision, Project administration. All authors have read and agreed to the published version of the manuscript.

Funding: This research was funded by the Scientific and Technological Research Council of Türkiye (TÜBİTAK) under the BİDEB-2232 program with grant number 118C311.

Data Availability Statement: Data is contained within the article.

Acknowledgments: The Center for Materials Research at İzmir Institute of Technology is gratefully acknowledged for the sample analyses.

Conflicts of Interest: The authors declare that they have no known competing financial interests or personal relationships that could have appeared to influence the work reported in this paper.

References

1. Zadbuke, N.; Shahi, S.; Gulecha, B.; Padalkar, A.; Thube, M. Recent trends and future of pharmaceutical packaging technology. *J. Pharm. Bioallied Sci.* **2013**, *5*, 98–110. [CrossRef] [PubMed]
2. Das, P.S.; Sah, P.; Das, R. Pharmaceutical packaging technology: A brief outline. *Res. J. Pharm. Dos. Forms Technol.* **2018**, *10*, 23–28. [CrossRef]

3. Pilchick, R. Pharmaceutical Blister Packaging. Part 1. *Pharm. Technol.* **2000**, *24*, 68–78.
4. Sonyy, S.M.; Chowdhury, H.; Loganathan, B.; Mustary, I.; Alam, F.; Tippayawong, N. Waste to Energy by Incineration for a Pharmaceutical Industry: A Case Study. In Proceedings of the 3rd International Conference on Energy and Power, ICEP2021, Chiang Mai, Thailand, 18–20 November 2021; American Institute of Physics Inc.: College Park, MD, USA, 2022. [\[CrossRef\]](#)
5. Kadam, A.; Patil, S.; Patil, S.; Tumkur, A. Pharmaceutical Waste Management An Overview. *Indian J. Pharm. Pract.* **2016**, *9*, 2–8. [\[CrossRef\]](#)
6. Çapkın, İ.Y.; Göknelma, M. Characterization and Separation Behavior of Multi-layers in Aluminum-Rich Waste Pharmaceutical Blisters. *JOM* **2023**, *75*, 4672–4679. [\[CrossRef\]](#)
7. Wang, B.; Yao, Z.; Reinmöller, M.; Kishore, N.; Tesfaye, F.; Luque, R. Pyrolysis behavior, kinetics, and thermodynamics of waste pharmaceutical blisters under CO₂ atmosphere. *J. Anal. Appl. Pyrolysis* **2023**, *170*, 105883. [\[CrossRef\]](#)
8. Klejnowska, K.; Pikoń, K.; Ścierański, W.; Skutil, K.; Bogacka, M. Influence of temperature on the composition and calorific value of gases produced during the pyrolysis of waste pharmaceutical blisters. *Appl. Sci.* **2020**, *10*, 737. [\[CrossRef\]](#)
9. Pikoń, K.; Ścierański, W.; Klejnowska, K.; Myćka, Ł.; Janoszka, A.; Sinek, A. Determination of fuel properties of char obtained during the pyrolysis of waste pharmaceutical blisters. *Energies* **2021**, *14*, 1782. [\[CrossRef\]](#)
10. Xu, B.; Argyle, M.D.; Shi, X.; Goroncy, A.K.; Rony, A.H.; Tan, G.; Fan, M. Effects of mixture of CO₂/CH₄ as pyrolysis atmosphere on pine wood pyrolysis products. *Renew. Energy* **2020**, *162*, 1243–1254. [\[CrossRef\]](#)
11. Armenise, S.; SyieLuing, W.; Ramírez-Velásquez, J.M.; Launay, F.; Wuebben, D.; Ngadi, N.; Rams, J.; Muñoz, M. Plastic waste recycling via pyrolysis: A bibliometric survey and literature review. *J. Anal. Appl. Pyrolysis* **2021**, *158*, 105265. [\[CrossRef\]](#)
12. Shen, Y.; Ma, D.; Ge, X. CO₂-looping in biomass pyrolysis or gasification. *R. Soc. Chem.* **2017**, *1*, 1700–1729. [\[CrossRef\]](#)
13. Steglich, J.; Dittrich, R.; Rombach, G.; Rosefort, M.; Friedrich, B.; Pichat, A. Dross Formation Mechanisms of Thermally Pre-Treated Used Beverage Can Scrap Bales with Different Density. In *Minerals, Metals and Materials Series*; Springer International Publishing: Cham, Switzerland, 2017; pp. 1105–1113. [\[CrossRef\]](#)
14. Diaz, F.; Flerus, B.; Nagraj, S.; Bokelmann, K.; Stauber, R.; Friedrich, B. Comparative Analysis About Degradation Mechanisms of Printed Circuit Boards (PCBs) in Slow and Fast Pyrolysis: The Influence of Heating Speed. *J. Sustain. Metall.* **2018**, *4*, 205–221. [\[CrossRef\]](#)
15. Pang, E.; Liu, W.; Zhang, S.; Fu, N.; Tian, Z. Characteristics of low-temperature polyvinyl chloride carbonization by catalytic CuAl layered double hydroxide. *Processes* **2020**, *8*, 120. [\[CrossRef\]](#)
16. Cruz, P.P.R.; da Silva, L.C.; Fiuza-Jr, R.A.; Polli, H. Thermal dehydrochlorination of pure PVC polymer: Part I—Thermal degradation kinetics by thermogravimetric analysis. *J. Appl. Polym. Sci.* **2021**, *138*, 50598. [\[CrossRef\]](#)
17. Zhu, T.; Yang, X.; He, X.; Zheng, Y.; Luo, J. Aromatic polyamides and copolyamides containing fluorene group: Synthesis, thermal stability, and gas transport properties. *High Perform. Polym.* **2018**, *30*, 821–832. [\[CrossRef\]](#)
18. Jung, M.R.; Horgen, F.D.; Orski, S.V.; Rodriguez, C.V.; Beers, K.L.; Balazs, G.H.; Jones, T.T.; Work, T.M.; Brignac, K.C.; Royer, S.-J.; et al. Validation of ATR FT-IR to identify polymers of plastic marine debris, including those ingested by marine organisms. *Mar. Pollut. Bull.* **2018**, *127*, 704–716. [\[CrossRef\]](#) [\[PubMed\]](#)
19. Higgins, F.; Zieschang, F. *Pharmaceutical Packaging Materials Quality Control and USP Chapter <661.1> Compliance*; Agilent: Santa Clara, CA, USA, 2021.
20. Zięba-Palus, J. The usefulness of infrared spectroscopy in examinations of adhesive tapes for forensic purposes. *Forensic Sci. Criminol.* **2017**, *2*, 1–9. [\[CrossRef\]](#)
21. Buch, V.; Mohamed, F.; Parrinello, M.; Devlin, J.P. Elusive structure of HCl monohydrate. *J. Chem. Phys.* **2007**, *126*, 074503. [\[CrossRef\]](#)
22. Nieminen, J.; Anugwom, I.; Kallioinen, M.; Mänttari, M. Green solvents in recovery of aluminium and plastic from waste pharmaceutical blister packaging. *Waste Manag.* **2020**, *107*, 20–27. [\[CrossRef\]](#)
23. Chen, Y.; Zhang, S.; Han, X.; Zhang, X.; Yi, M.; Yang, S.; Yu, D.; Liu, W. Catalytic Dechlorination and Charring Reaction of Polyvinyl Chloride by CuAl Layered Double Hydroxide. *Energy Fuels* **2018**, *32*, 2407–2413. [\[CrossRef\]](#)
24. Ramesh, S.; Leen, K.H.; Kumutha, K.; Arof, A.K. FTIR studies of PVC/PMMA blend based polymer electrolytes. *Spectrochim. Acta A Mol. Biomol. Spectrosc.* **2007**, *66*, 1237–1242. [\[CrossRef\]](#) [\[PubMed\]](#)
25. Diaz, F.; Latacz, D.; Friedrich, B. Enabling the recycling of metals from the shredder light fraction derived from waste of electrical and electronic equipment via continuous pyrolysis process. *Waste Manag.* **2023**, *172*, 335–346. [\[CrossRef\]](#) [\[PubMed\]](#)
26. Dittrich, R.; Friedrich, B.; Rombach, G.; Steglich, J.; Pichat, A. Understanding of Interactions Between Pyrolysis Gases and Liquid Aluminum and Their Impact on Dross Formation. In *The Minerals, Metals & Materials Series*; Springer International Publishing: Cham, Switzerland, 2017; pp. 1457–1464.
27. Magomedov, R.N.; Nikitin, A.V.; Savchenko, V.I.; Arutyunov, V.S. Production of gas mixtures with regulated ratios between ethylene and carbon monoxide by the gas-phase oxidative cracking of light alkanes. *Kinet. Catal.* **2014**, *55*, 556–565. [\[CrossRef\]](#)
28. Scholz, R.; Beckmann, M.; Schulenburg, F. *Abfallbehandlung in Thermischen Verfahren*; Vieweg+Teubner Verlag Wiesbaden: Wiesbaden, Germany, 2001.
29. Msheik, M.; Rodat, S.; Abanades, S. Methane cracking for hydrogen production: A review of catalytic and molten media pyrolysis. *Energies* **2021**, *14*, 3107. [\[CrossRef\]](#)
30. Gai, W.Z.; Fang, C.S.; Deng, Z.Y. Hydrogen generation by the reaction of Al with water using oxides as catalysts. *Int. J. Energy Res.* **2014**, *38*, 918–925. [\[CrossRef\]](#)

31. Basu, P. *Biomass Gasification and Pyrolysis: Practical Design and Theory*; Academic Press: Cambridge, MA, USA, 2010.
32. Kurzweil, P. Grundlagen, Komponenten, Systeme, Anwendungen. In *Brennstoffzellentechnik*, 2nd ed.; Springer: Wiesbaden, Germany, 2013.

Disclaimer/Publisher's Note: The statements, opinions and data contained in all publications are solely those of the individual author(s) and contributor(s) and not of MDPI and/or the editor(s). MDPI and/or the editor(s) disclaim responsibility for any injury to people or property resulting from any ideas, methods, instructions or products referred to in the content.